SAW filter manufacture and piezoelectric materials evaluation based on printed electronics technology*

LIU Xiao-chen (刘晓辰)**, LI Kun** (李琨)****, XUAN Xiu-wei** (轩秀巍)**, CAO Yang** (曹阳)**, and TENG Jian-fu** (滕建辅)

Tianjin Key Laboratory of Film Electronic and Communication Device, School of Electronics Information Engineering, Tianjin University of Technology, Tianjin 300384, China

(Received 19 June 2014)

In this paper, the silver nanoparticle ink and ink-jet printing technology are used to manufacture the surface acoustic wave (SAW) filters. The characteristics of three common substrate piezoelectric materials of ST-quartz, Y36° -$LiTaO_3$ and Y128°-$LiNbO_3$ are evaluated. The experimental results show that Y128°-$LiNbO_3$ matches the ink much better than others. The printed SAW filter with Y128°-$LiNbO_3$ as piezoelectric substrate is realized, and its center frequency and bandwidth are 18.4 MHz and 500 kHz, respectively.

Document code: A **Article ID:** 1673-1905(2014)05-0340-3

DOI 10.1007/s11801-014-4117-4

Printed electronics (PE) is a rapidly developing field. Both organic and inorganic materials are used for printed electronics[1-6]. In the field of the organic materials, a lot of methods have been proposed to prepare organic field-effect transistors (OFETs) and organic light-emitting diodes (OLEDs). In 2013, a fast-switching organic electrochemical transistor was implemented with all-printed technologies[7]. And Baeg et al[8] have printed both p-type and n-type OFETs, with which high-performance inverters and various digital logic gates, such as NAND, NOR, OR and XOR, are realized on flexible plastic substrates. The organic materials were also used to print matrix addressed display[9,10]. One of the most used inorganic materials is metal nanoparticle ink which offers lower conductivity. For example, silver nanoparticle ink has been widely used for manufacturing radio frequency identification (RFID) tags. In 2014, Henrik A. Andersson[11] investigated hybrid printed electronics, where components of regular surface mount technology (SMT) are mounted on printed flexible substrates to achieve high functionality at a low cost.

In this paper, applying PE technology to manufacture the surface acoustic wave (SAW) devices is proposed. There are two reasons for applying PE. Firstly, the structure of SAW filter is simple, which is mainly composed of a piezoelectric substrate and a flat metal with particular pattern on the top. Secondly, the PE technology is good at defining patterns on substrates, and the metal nanoparticle ink has been widely used for printing conductive layers. Compared with the conventional processes, such as sputtering, evaporation and lithography, the PE technology has many advantages, namely, the equipment for PE is not very expensive, no waste water or gas is generated, and the process is much simpler.

The SAW filter, which is one kind of typical SAW devices, is chosen to be fabricated with PE technology in this paper. The main part of SAW filter is the interdigital transducer (IDT) as shown in Fig.1(a). In order to simplify the design, the width of electrodes a and spacing between electrodes b are equal to each other, i.e., a=b=50 μm. The parameter w which means the width of aperture is designed as 4 000 μm, and the distance between two IDTs is 6 000 μm. Each IDT has 30 pairs of interdigital electrodes. Fig.1(b) shows the full view of the SAW filter's layout.

In the printing procedure, the substrates should be cleaned with acetone solution, then the pattern of IDT is printed with ink-jet printing machine and silver nano-particle ink, and lastly the printed devices are heated in a convection oven at 120 °C for 5 min.

Furthermore, the characteristics for three substrate materials of ST-quartz, Y36°-$LiTaO_3$ and Y128°-$LiNbO_3$ are evaluated. All substrates with thickness of 0.43 mm are polished on one side. Since different kinds of substrates have different surface energy, their printing performances have obvious difference. Fig.2 shows the images of printed SAW filters with three kinds of substrates.

Because the surface energy of the substrates with ST-quartz and Y36°-$LiTaO_3$ does not match the ink, the printed pattern on the substrate of ST-quartz shrinks obviously to several droplets as shown in Fig.2(a), and the edges of the printed electrodes are not clear on the Y36°-$LiTaO_3$ as shown in Fig.2(b). However, the pattern

* This work has been supported by the Project of the Science & Technology Pillar Program of Tianjin (No.12ZCZDJC35500), and the Natural Science Foundation of Tianjin (No.13JCQNJC01300).

** E-mail: likun_tjut@163.com

of the IDT is clear in Fig.2(c), which indicates that the substrate of Y128°-$LiNbO_3$ matches the ink very well. Fig.3 shows the photo of the completed printed SAW filter on the substrate of Y128°-$LiNbO_3$.

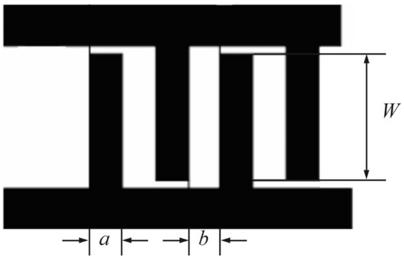

(a) The structure parameters in IDT

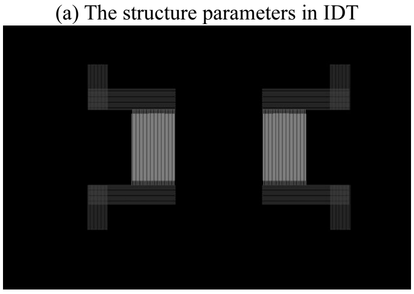

(b) The full view of IDT

Fig.1 The detailed drawing and AutoCAD drawing of IDT

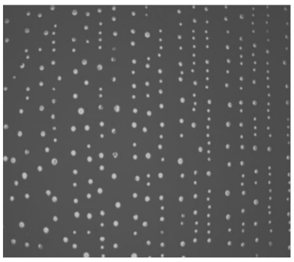

(a) With quartz as substrate

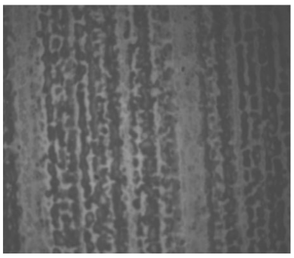

(b) With $LiTaO_3$ as substrate

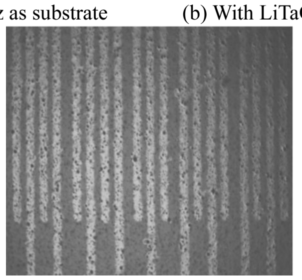

(c) With $LiNbO_3$ as substrate

Fig.2 The microscope images of printed SAW filters with different substrates

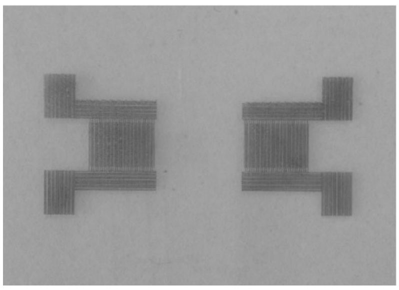

Fig.3 The photo of the printed SAW filter on the substrate of Y128°-$LiNbO_3$

Then the performance of the SAW filter with $LiNbO_3$ as substrate is carefully investigated. In the first step, the electrodes of IDT are measured by electrical conductivity test. The experimental results show that the positive and negative inputs of the same IDT are not affected mutually, which indicates that the adjacent electrodes do not cross-connected.

In the second step, the amplitude frequency response of the SAW filter is simulated and measured. Based on the δ function model of SAW filter, the center frequency is calculated as

$$f_0=V_{\mathrm{SAW}}/4a. \quad (1)$$

The speed of the SAW spreading on the surface of Y128°-$LiNbO_3$ is about 3 960 m/s. According to the parameters of the IDT given in Fig.1(a), the center frequency of the printed SAW filter can be calculated as 19.6 MHz. The simulation result of amplitude-frequency characteristic of the filter is shown in Fig.4.

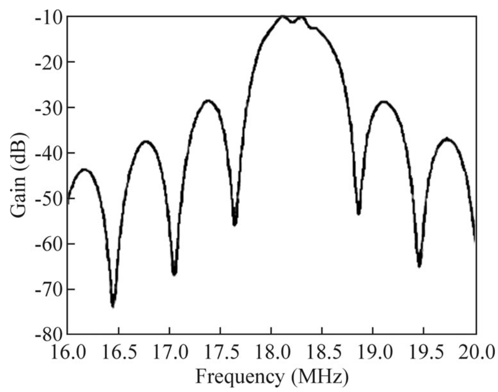

Fig.4 The simulation result of amplitude-frequency characteristic of the SAW filter

The simulation results show that the pass-band is about 18.0–18.5 MHz, the insertion loss of the pass-band is around 10.0 dB, and the minimum attenuation of the stop band is almost 30.0 dB.

With a signal source and an oscilloscope, the actual amplitude-frequency response of the printed SAW filter is tested. During the test, the signal source generates a sinusoidal wave signal with frequency f and amplitude A. This signal is sent into the SAW filter, and then the amplitude of output signal A' is measured by oscilloscope. The gain of the SAW filter at the frequency of f can be calculated as A'/A. As the signal source sweeps the band of the frequency, the amplitude-frequency characteristic of the SAW filter can be obtained. The measured result is shown in Fig.5.

The pass-band frequency of the SAW filter is 18.15–18.60 MHz, the maximum attenuation of pass-band is about 10.0 dB, the bands of transition in 17.60–18.00 MHz and 18.50–18.70 MHz are steep, and the minimum attenuation of the filter in stop-band is about 40 dB. The measured results are consistent with the simulation results shown in Fig.4.

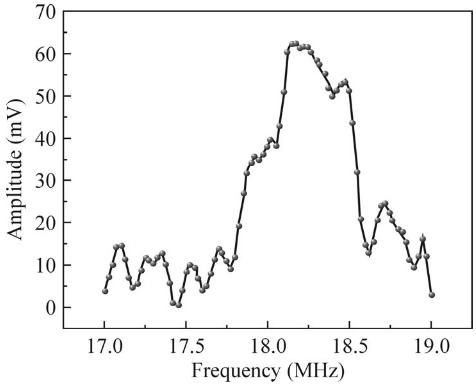

Fig.5 The measured amplitude-frequency characteristic of the SAW filter

In conclusion, the PE technology can be applied to manufacture the SAW devices, the substrate of Y128°-$LiNbO_3$ matches the silver nanoparticle ink very well, and the printed SAW filter on the substrate of Y128°-$LiNbO_3$ has great performance. Although the simulated result and the measured result agree very well, the characteristic of the filter is not so good, which is mainly due to the characteristic of the prototype of the designed SAW filter is not perfect. In the further research, the design of SAW filter for PE technology should be focused.

References

[1] S. K. Park, Y. H. Kim, J. I. Han, D. G. Moon and W. K. Kim, IEEE Transactions on Electron Devices **49**, 2008 (2002).

[2] H. Sirringhaus, T. Kawase, R. H. Friend, T. Shimoda, M. Inbasekaran, W. Wu and E. P. Woo, Science **290**, 2123 (2000).

[3] J. J. Schneider, R. C. Hoffmann, J. Engstler, O. Soffke, W. Jaegermann, A. Issanin and A. Klyszcz, Advanced Materials **20**, 3383 (2008).

[4] Y. Y. Noh, X. Y. Cheng, H. Sirringhaus, J. I. Sohn, M. E. Welland and D. J. Kang, Applied Physics Letters **91**, 043109 (2007).

[5] J. Vaillancourt, H. Y. Zhang, P. Vasinajindakaw, H. T. Xia, X. J. Lu, X. L. Han, D. C. Janzen, W. S. Shih, C. S. Jones, M. Stroder, M. Y. Chen, H. Subbaraman, R. T. Chen, U. Berger and M. Renn, Applied Physics Letters **93**, 243301 (2008).

[6] M. Harting, J. Zhang, D. R. Gamota and D. T. Britton, Applied Physics Letters **94**, 193509 (2009).

[7] P. A. Ersman, D. Nilsson, J. Kawahara, G. Gustafsson and M. Berggren, Organic Electronics **14**, 1276 (2013).

[8] K. J. Baeg, D. Khim, J. Kim, D. Y. Kim, S. W. Sung, B. D. Yang and Y. Y. Noh, IEEE Electron Device Letters **34**, 126 (2013).

[9] J. Kawahara, P. A. Ersman, D. Nilsson, K. Katoh, Y. Nakata, M. Sandberg, M. Nilsson, G. Gustafsson and M. Berggren, Journal of Polymer Science Part B: Polymer Physics **51**, 265 (2013).

[10] P. A. Ersman, J. Kawahara and M. Berggren, Organic Electronics **14**, 3371 (2013).

[11] H. A. Andersson, A. Manuilskiy, S. Haller, M. Hummelgard, J. Siden, C. Hummelgard, H. Olin and H. E. Nilsson, Nanotechnology **25**, 4002 (2014).